Adding static printing capabilities to the EUV phase-shifting point diffraction interferometer

Patrick Naulleau[1], Kenneth A. Goldberg[1], Erik H. Anderson[1], Phillip Batson[1], Paul Denham[1], Keith Jackson[1], Seno Rekawa[1], and Jeffrey Bokor[1,2]

[1]Center for X-Ray Optics, Lawrence Berkeley National Laboratory, Berkeley, CA 94720
[2]EECS Department, University of California, Berkeley, CA 94720

ABSTRACT

While interferometry is routinely used for the characterization and alignment of lithographic optics, the ultimate performance metric for these optics is printing in photoresist. Direct comparison of imaging and wavefront performance is also useful for verifying and improving the predictive power of wavefront metrology under actual printing conditions. To address these issues, static, small-field printing capabilities are being added to the extreme ultraviolet (EUV) phase-shifting point diffraction interferometer (PS/PDI) implemented at the Advanced Light Source at Lawrence Berkeley National Laboratory. This Sub-field Exposure Station (SES) will enable the earliest possible imaging characterization of the upcoming Engineering Test Stand (ETS) Set-2 projection optics.

Relevant printing studies with the ETS projection optics require illumination partial coherence with σ of approximately 0.7. This σ value is very different from the coherent illumination requirements of the EUV PS/PDI and the coherence properties naturally provided by synchrotron undulator beamline illumination. Adding printing capabilities to the PS/PDI experimental system thus necessitates the development of an alternative illumination system capable of destroying the inherent coherence of the beamline. The SES is being implemented with two independent illuminators: the first is based on a novel EUV diffuser currently under development and the second is based on a scanning mirror design.

Here we describe the design and implementation of the new SES, including a discussion of the illuminators and the fabrication of the EUV diffuser.

Keywords: extreme ultraviolet lithography, synchrotron radiation, microfield printing, EUV diffuser, decoherentizing illuminator

1. INTRODUCTION

The semiconductor industry's push towards ever-smaller circuit feature sizes has led to a continual shortening of the wavelength used in the lithography step. Historically, lithography systems used in mass production have been based on refractive projection optical systems. However, continuation of the wavelength-shortening trend and the unavailability of transparent refractive materials for shorter wavelengths will eventually lead to a departure from refractive systems. One of the most promising so-called *next-generation lithography* systems is extreme ultraviolet (EUV) projection lithography, in which multilayer-coated mirrors are used to form compound projection optics operating in the 13- to 14-nm wavelength range. Achieving lithographic-quality, diffraction-limited performance requires that the projection optics have rms wavefront quality on the order of $\lambda/50$ (0.27 nm at λ = 13.4 nm).[1] Because EUV systems utilize resonant reflective coatings,[2] at-wavelength characterization[3] is critical to the development process.

In order to meet the at-wavelength wavefront metrology challenge, an EUV-compatible diffraction-class interferometer, the phase-shifting point diffraction interferometer (PS/PDI), was developed by Medecki *et al.*[4] The PS/PDI is a common-path, system-level interferometer that relies on pinhole diffraction to generate both the illumination and reference beams. A diffraction grating is used as the beam-splitting and phase-shifting element. The PS/PDI has recently been demonstrated to have a reference wavefront accuracy of better than $\lambda_{EUV}/350$ (0.4 Å) within a numerical aperture (NA) of 0.082.[5]

The EUV PS/PDI, implemented at Lawrence Berkeley National Laboratory's Advanced Light Source synchrotron radiation facility, has been in operation for several years and is routinely used to characterize EUV lithographic optics.[6-8] Two separate EUV PS/PDI interferometers have been constructed: the first was designed to test the 10×-reduction EUV Schwarzschild cameras[9] used in the Microsteppers[10] installed at Sandia National Laboratories whereas the second, much larger scale interferometer, was designed to test the 4×-reduction projection optics box[11] designed at Lawrence Livermore National Laboratory and used in the EUV Engineering Test Stand (ETS)[12] now operational at the Virtual National Laboratory (the Virtual National Laboratory is a partnership between Lawrence Berkley, Lawrence Livermore, and Sandia National Laboratories).

While wavefront interferometry is routinely used for the characterization and alignment of lithographic optics, the ultimate performance metric is printing in photoresist. Direct comparison of imaging and wavefront performance is also useful for verifying and improving the predictive power of wavefront metrology under actual printing conditions. To address these issues, static, small-field printing capabilities are being added to the EUV PS/PDI designed to characterize ETS projection optics. Although the ultimate destination for these optics remains integration into the ETS for full-field scanned imaging, valuable early learning can be obtained by the new small-field static printing capabilities of the enhanced PS/PDI endstation. This Sub-field Exposure Station (SES) will enable the earliest possible imaging characterization of the ETS set-2 projection optics (undergoing final assembly as of the writing of this manuscript, February, 2001).

A static imaging system, the SES will have a subfield size of approximately 100 μm at the wafer. However, the full 1-inch arc field can be covered one subfield at a time by moving the entire system relative to the stationary illumination beam as is done in the interferometry.[13] The SES will work with essentially the same reflection masks as used in the ETS. In addition, the SES will support variable partial coherence (σ) ranging from approximately 0.2 to 1.

The biggest challenge for the implementation of printing capabilities at the EUV interferometry beamline is illumination coherence. Relevant printing studies with the ETS projection optics require illumination partial coherence (σ) of approximately 0.7. This σ value is very different from the coherent illumination requirements of the EUV PS/PDI and the coherence properties naturally provided by synchrotron undulator beamline illumination.[14,15] Adding printing capabilities to the PS/PDI experimental system thus necessitates the development of an alternative illumination system capable of destroying the inherent coherence of the beamline. The SES is being implemented with two independent illuminators: the first is based on a novel EUV diffuser currently under development and the second is based on a scanning mirror design.

2. ADDING PRINTING CAPABILITIES TO THE PS/PDI

Although the illumination issue is the most fundamental of the changes required to implement printing in the EUV interferometry tool, several other modifications are necessary. In this section we summarize these modifications; the illumination is specifically addressed in the next section.

By design, the PS/PDI (Fig. 1) is a transmission device. The beamline illumination comes from above where it is focussed onto a subresolution pinhole in the object (reticle) plane of the

optic under test. Transmission through this pinhole serves to generate an ideally spherical interferometric probe beam. This probe beam is then split into multiple beams by transmission through a grating: one of the beams eventually serves as the interferometric reference.

In contrast to the transmission configuration of the interferometry, relevant printing studies require a reflection mask (reticle) to be used and, therefore, the illumination must come from below. This is achieved by providing clearance for the beam to pass downward through the object plane before it is redirected upward to illuminate the reflection reticle (Fig. 2). Because the grating is not required for imaging, the optic used to redirect the beam upward can be conveniently positioned at the location of the grating. This allows the same stage configuration to be used in both the interferometry and imaging modes. Switching between modes simply requires the two stages to be interchanged.

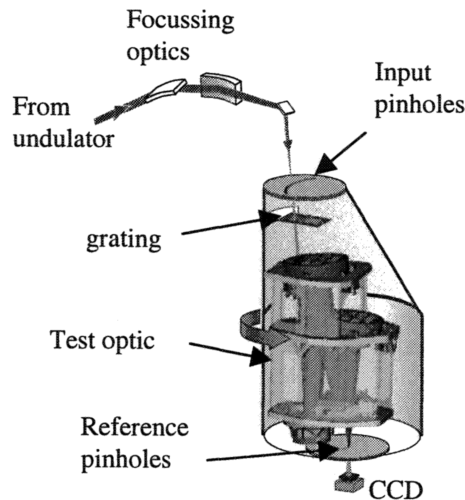

Fig. 1. Schematic of PS/PDI endstation in interferometry mode. Beamline illumination is focussed to the object plane from above where transmission through a subresolution pinhole generates the spherical probe beam.

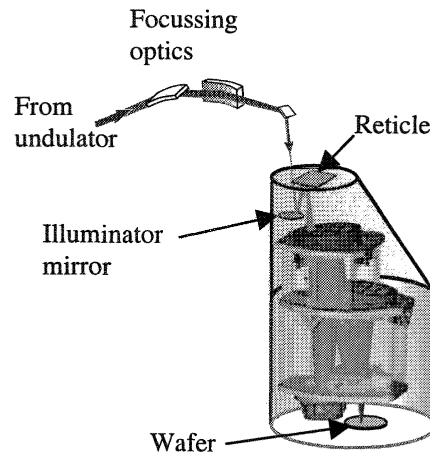

Fig. 2. Schematic of PS/PDI endstation in SES mode. Beamline illumination passes through the object plane and is redirected upward using mirror that replaces grating used in interferometry mode.

The SES configuration shown in Fig. 2 provides for a 19-mm clearance in the object plane between the incoming beam and the illumination spot on the reticle. This clearance is set by the angles of incidence (5.4°) and the distance from the final illuminator mirror to the object plane. Because the optic field of view is arc shaped, this limited clearance requires the reticle pattern to be as close as 4 mm from the reticle edge at the apex of the arc. Due to the fabrication difficulties involved in multilayer coating and patterning so close to the edge, the pattern is instead placed near the center of a 6-inch square reticle which is subsequently cut.

Another important issue for the SES is image-plane-stage speed. The original flexural, picomotor-driven stage design was optimized for extremely high resolution (better than 10 nm) at the expense of speed (the original stage speed was approximately 1 μm per second). This resolution is essential for positioning of the image-plane pinhole used to generate the interferometric reference beam. In static imaging mode, however, stage resolution is not important, whereas stage speed is. Without improvement of the stage speed, focus–exposure matrix acquisition times would be largely dominated by stage positioning time.

To address the lateral-scanning speed issue a nested-stage solution has been implemented (Fig. 3). The entire picomotor drive assembly is now separately driven by a much faster, optical-positioning DC-servo motor providing an approximately 20× increase in stage speed. This nested design allows the same stage to be used in both interferometry and printing modes, facilitating the transition between the two modes.

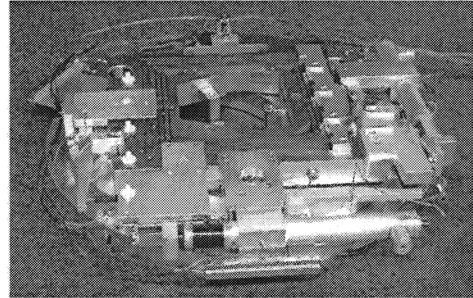

Fig. 3. Dual-mode image-plane stage. This is a flexural stage with picomotor drive for high resolution in interferomety mode and nested DC-servo drive for high speed in printing mode.

The new image-plane stage is also equipped with an electrostatic chuck to hold the imaging wafers flat. In orer to accommodate interferometry, the chuck has an open slot in the area of the static field through which the interferometric beams pass to the CCD.

The other major mechanical upgrade for printing functionality is the addition of a vacuum load-lock wafer-transfer system for the image-plane stage. This custom-designed system enables rapid transfer of imaging wafers and provides adequate positioning accuracy for the pinhole wafers used in interferometry mode.

3. ILLUMINATORS

As stated above, two illumination systems are being implemented for the SES. The first is based on a novel EUV diffuser currently under development. Although encouraging progress has been made in the development of this diffuser, a final device of acceptable efficiency has yet to be fabricated. Thus, we have concurrently developed a second illuminator based on a scanning mirror design. The two illuminators can be implemented in parallel, and switching from one to the other is relatively trivial.

The diffuser-based illuminator was particularly attractive for the SES because of its simple mechanical implementation facilitating integration into the existing PS/PDI and ease of coherence tuning. Figure 4 shows a schematic of this illuminator. It utilizes a single reflective diffraction element serving as the EUV analog to "ground glass" in a visible-light system.[16] To actually decoherentize the illumination, the diffuser must be actively moved relative to the beam. This has been accomplished by placing the diffuser on a rotating platter operating at 100 revolutions per minute.

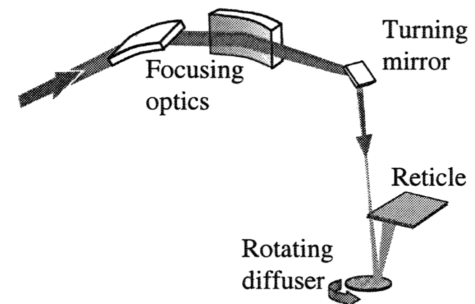

Fig. 4. Diffuser-based illuminator for SES. Implemented using single reflective diffraction element. The diffuser is an EUV analog of "ground glass" in a visible-light system.

The reflective diffuser also serves to redirect the beam upward. The diffuser acts as a new illumination source whose size can be changed by changing the illumination area on the diffuser. Because this system is effectively Köhler within our limited field size of approximately 400 μm at the reticle, the illumination can be treated as stationary. Moreover, the illumination coherence can be controlled by changing the illumination area on the diffuser.

The illumination size and uniformity at the reticle depend in large part on the scattering characteristics of the diffuser. Thus, efficient performance relies on accurate control of the diffuser scattering properties.

An EUV diffuser can be fabricated by coating a rough surface with a conventional EUV reflective multilayer (Fig. 5). In order to achieve adequate efficiency, however, the starting roughness of the substrate must be well controlled in both amplitude and spatial-frequency bandwidth. Experience has shown naturally-rough substrates to be inadequate for this purpose. Instead we use substrates of engineered roughness patterned into a layer of photoresist.

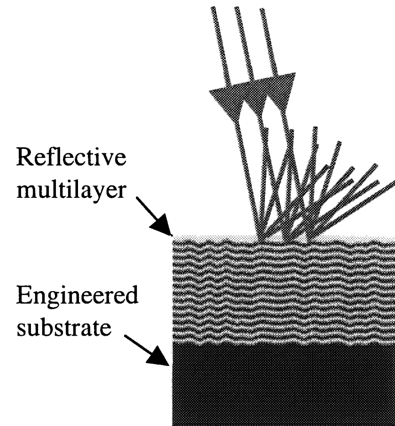

Fig. 5. EUV diffuser fabricated by coating engineered rough substrate with conventional EUV reflective multilayer.

The roughness patterning is achieved by way of a grayscale e-beam exposure of the resists followed by a developing step in which the resist is only partially cleared. In this way, exposure dose is mapped to remaining resist thickness and arbitrary relief profiles can be generated. The resist relief profile is then overcoated with a multilayer to created the EUV diffuser. We have found glass-based resists to be particularly well suited to this application due to their post-development stability.

To facilitate development and calibration of the diffuser fabrication process, we have worked with 5-level sawtooth grating structures (depicted schematically in Fig. 6). For the SES configuration, the diffuser lateral feature size should be in the 200- to 500-nm range and the total peak-to-valley height should be approximately 24 nm. Accordingly, we designed the development gratings to be comprised of steps that are 250-nm wide and of various heights bracketing the target height of 24 nm.

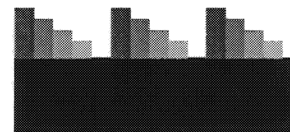

Fig. 6. Diffuser-fabrication calibration profile.

Using the method described above, numerous development gratings ranging in height from 3 to 35 nm have been fabricated. Figure 7 shows atomic force microscope (AFM) images of a typical one of these gratings. Figure 7(a) shows the resist profile, 7(b) shows the profile after multilayer coating, and 7(c) shows the average profile after coating (the averaging was performed along the direction of the grating lines). The desired relief structure has been successfully transferred to the resist and the structure preserved through the multilayer-coating process.

We note that the multilayer smoothing effect[17] is not of concern here due to the relatively large lateral feature sizes; however, smoothing of the higher-frequency intrinsic resist roughness seen in Fig. 7(a) is evident. Although beneficial for our purposes, the smoothing seen going from Fig 7(a) to (b) is not sufficient to counter the deleterious effects of the roughness on the diffuser efficiency. An rms roughness of greater than 1.5 nm remains in Fig. 7(b). A factor of three reduction or better is still required. Various process enhancements aimed at reducing this intrinsic

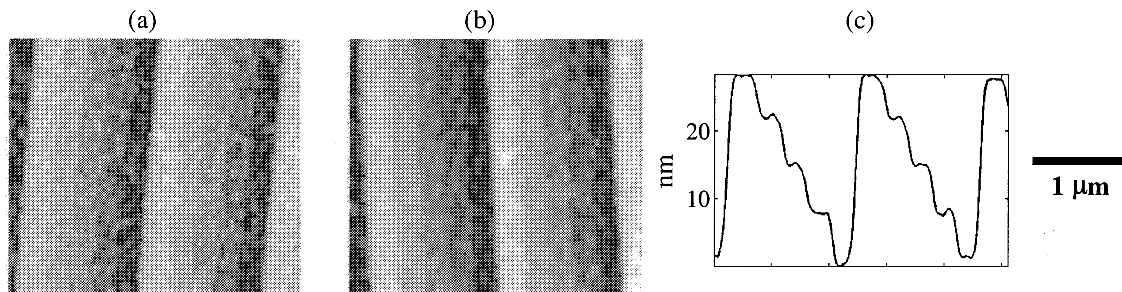

Fig. 7. (a) Atomic force microscope (AFM) image of engineered substrate based on sawtooth calibration profile. (b) AFM image after multilayer coating. (c) Average profile after coating (profile averaged along direction of grating lines). Lighter regions in the image represent taller areas on the sample.

resist roughness are currently under investigation.

To mitigate our risk of failing to produce a diffuser of adequate efficiency, we have also implemented a scanning-mirror illuminator for the SES, shown schematically in Fig. 8. In this case, we replace the rotating diffuser with a stationary spherical mirror selected to re-image the scanning turning mirror to the reticle. The turning mirror is scanned in angle in two dimensions, thereby, synthesizing the pupil-fill pattern. Re-imaging the scanning mirror to the reticle ensures that each point on the reticle sees all illumination angles. By adjusting the scan-angle magnitude, this system is also capable of *in situ* σ control. Being a critical illuminator, a possible drawback of this system is increased sensitivity to spatial intensity variations on the turning mirror and in the incoming beam.

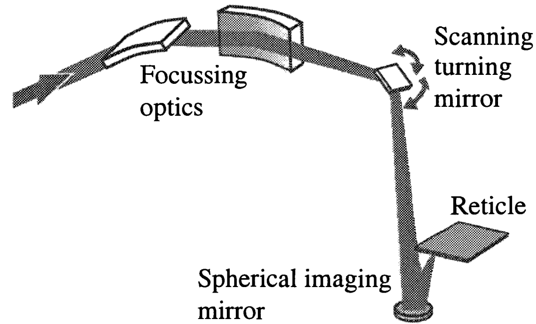

Fig. 8. Schematic of scanning-mirror SES illuminator. The diffuser is replaced by a spherical mirror that re-images the scanning turning mirror to the reticle. The turning mirror is scanned in angle in two dimensions, thereby, synthesizing the pupil-fill pattern.

SUMMARY

The EUV PS/PDI recently implemented to characterize and align ETS optics has been upgraded to support small-field static printing experiments in addition to wavefront metrology. This system, planned for use in Summer 2001, will enable the earliest possible imaging demonstration with the new ETS Set-2 optics (undergoing final assembly as of the writing of this manuscript, February 2001). The SES will also enable the direct comparison of imaging and wavefront performance, useful for verifying and improving the predictive power of wavefront metrology under actual printing conditions.

To accurately replicate realistic printing conditions, it is crucial that the inherent coherence of the EUV interferometry beamline be reduced. Two separate illuminators achieving this goal have been implemented: the first is based on a novel EUV diffuser currently under development and the second is based on a scanning mirror design. We note that the diffuser technology being developed here can be quite generally applicable to the fabrication of diffractive optical elements in the EUV wavelength range. Such components may have many applications in EUV lithography, such as in the more complex illuminators to be used in full-field steppers.

ACKNOWLEDGEMENTS

The authors are greatly indebted to Kevin Bradley, Rene Delano, Bruce Harteneck, Brian Hoef, Gideon Jones, Drew Kemp, David Richardson, Farhad Salmassi, Ron Tackaberry, and Eugene Veklerov for expert engineering and fabrication support, and to the entire CXRO staff for enabling this research. This research was supported by the Extreme Ultraviolet Limited Liability Company and the DOE Office of Basic Energy Science.

REFERENCES

1. D. M. Williamson, "The elusive diffraction limit," *OSA Proceedings on Extreme Ultraviolet Lithography*, F. Zernike and D. T Attwood, eds. (Optical Society of America, Washington, DC 1995), Vol. **23**, pp. 68-76.
2. J. H. Underwood and T. W. Barbee, Jr., "Layered synthetic microstructures as Bragg diffractors for X rays and extreme ultraviolet: theory and predicted performance," Appl. Opt. **20**, 3027-3034 (1981).

3. D. Attwood, G. Sommargren, R. Beguiristain, K. Nguyen, J. Bokor, N. Ceglio, K. Jackson, M. Koike, and J. Underwood, "Undulator radiation for at-wavelength interferometry of optics for extreme-ultraviolet lithography," Appl. Opt. **32**, 7022-7031 (1993).

4. H. Medecki, E. Tejnil, K. A. Goldberg, and J. Bokor, "Phase-shifting point diffraction interferometer," Opt. Lett. **21**, 1526-1528 (1996).

5. P. Naulleau, K. Goldberg, S. Lee, C. Chang, D. Attwood, and J. Bokor, "Extreme-ultraviolet phase-shifting point diffraction interferometer: a wave-front metrology tool with sub-angstrom reference-wave accuracy," Appl. Opt. **38**, 7252-7263 (1999).

6. K. A. Goldberg, E. Tejnil, S. H. Lee, H. Medecki, D. T. Attwood, K. H. Jackson, and J. Bokor, "Characterization of an EUV Schwarzschild objective using phase-shifting point diffraction interferometry," Proc. SPIE Vol. **3048**, 264-70 (1997).

7. K. A. Goldberg, P. Naulleau, and J. Bokor, "EUV interferometric measurements of diffraction-limited optics," J. Vac. Sci. and Technol. B **17**, 2982-86 (1999).

8. K. A. Goldberg, P. Naulleau, P. Batson, P. Denham, H. Chapman, and J. Bokor, "Extreme ultraviolet alignment and testing of a four mirror aspheric extreme ultraviolet optical system," J. Vac. Sci. and Technol. B **18**, 2911-15 (2000).

9. D. A. Tichenor, G. D. Kubiak, M. E. Malinowski, R. H. Stulen, S. J. Haney, K. W. Berger, R. P. Nissen, R. L. Schmitt, G. A. Wilkerson, L. A. Brown, P. A. Spence, P. S. Jin, W. C. Sweat, W. W. Chow, J. E. Bjorkholm, R. R. Freeman, M. D. Himel, A. A. MacDowell, D. M. Tennant, O. R. Wood II, W. K. Waskiewicz, D. L. White, D. L. Windt, and T. E. Jewell, "Development and characterization of a 10× Schwarzschild system for SXPL," in *OSA Proceedings on Soft X-Ray Projection Lithography,* Vol. **18**, A. M. Hawryluk and R. H. Stulen, eds., (Optical Society of America, Washington, DC, 1993), pp. 79-82.

10. J. Goldsmith, K Berger, D. Bozman, G. Cardinale, D. Folk, C. Henderson, D. O'Connell, A. Ray-Chaudhuri, K. Stewart, D. Tichenor, H. Chapman, R. Gaughan, R. Hudyma, C. Montcalm, E. Spiller, J. Taylor, J. Williams, K. Goldberg, E. Gullikson, P. Naulleau, and J. Cobb, "Sub-100-nm imaging with an EUV 10x microstepper," Proc. SPIE **3676**, 264-271 (1999).

11. D. W. Sweeney, R. Hudyma, H. N. Chapman, and D. Shafer, "EUV optical design for a 100 nm CD imaging system," in *Emerging Lithographic Technologies II*, Y. Vladimirsky, ed., Proc. SPIE **3331**, 2-10 (1998).

12. D. Tichenor, G. Kubiak, W. Replogle, L. Klebanoff, J. Wronosky, L. Hale, H. Chapman, J. Taylor, J. Folta, C. Montcalm, R. Hudyma, K. Goldberg, and P. Naulleau, "EUV Engineering Test Stand," Proc. SPIE **3997**, 48-69 (2000).

13. K. A. Goldberg, P. Naulleau, P. J. Batson, P. Denham, J. Bokor, and H. N. Chapman, "EUV Interferometry of a Four-mirror Ring Field EUV Optical System," Proc. SPIE **3997**, 867-873 (2000).

14. D. Attwood, P. Naulleau, K. Goldberg, E. Tejnil, C. Chang, R. Beguiristain, P. Batson, J. Bokor, E. Gullikson, H. Medecki, and J. Underwood, "Tunable coherent radiation in the soft X-ray and extreme ultraviolet spectral regions," IEEE J. Quantum Electron. **35**, 709-720 (1999).

15. C. Chang, P. Naulleau, E. Anderson, and D. Attwood, "Spatial coherence characterization of undulator radiation," Opt. Comm. **182**, 25-34 (2000).

16. J. W. Goodman, *Statistical Optics*, John Wiley & Sons, New York, 1986.

17. D. G. Stearns, "Stochastic model for thin film growth and erosion," Appl. Phys. Lett. **62**, 1745-1747, (1993).